Available online at www.sciencedirect.com
SCIENCE DIRECT®
Marine Geology 204 (2004) 187–202
MARINE GEOLOGY
INTERNATIONAL JOURNAL OF MARINE GEOLOGY, GEOCHEMISTRY AND GEOPHYSICS
www.elsevier.com/locate/margeo

Morphological evolution and time-varying bedrock control of main channel at a mixed energy tidal inlet: Maumusson Inlet, France

Xavier Bertin [a,*], Eric Chaumillon [a], Nicolas Weber [b], Michel Tesson [c]

[a] *Centre Littoral de Géophysique, Université de La Rochelle, Avenue Michel Crépeau, 17042 La Rochelle cedex 1, France*
[b] *EPSHOM, Cellule sédimentologie, 13 rue des Chateliers, B.P. 30316, 29603 Brest cedex, France*
[c] *Université de Perpignan, 66860 Perpignan, France*

Received 15 January 2003; received in revised form 7 October 2003; accepted 11 November 2003

Abstract

Maumusson Inlet, located on the French Atlantic coast, connects the Atlantic Ocean with the Marennes–Oléron tidal bay. The tidal range (2–6 m) and wave climate (mean height 1.5 m) place this tidal inlet in the mixed energy, tide dominant, category of Hayes [(1979) Barrier island morphology. In: Leatherman, S.P. (Ed.), Barrier Island, Academic Press, New York, pp. 1–28]. An innovative method, combining high quality bathymetric data (nine accurate Digital Elevation Models since 1824) with a very high seismic resolution, demonstrates a major tidal inlet evolution from 1824 onwards and its dramatic acceleration since 1970. The chronology of those morphological changes suggests strong coupling between the location of the tidal channel and the behaviour of the adjacent shorelines. The recent shoaling and migration of the inlet channel can be attributed to a decrease in tidal prism due to the filling in sediment of Marennes–Oléron Bay. Seismic data give evidence that the inlet was located on a major incision of the bedrock. It can be inferred that the bedrock exerts control of channel location, this control varying in time as a function of channel depth. A conceptual model is proposed, including the inlet, its adjacent shorelines, the tidal bay and the time-varying bedrock control of main channel location. Such a model could be considered valid in similar cases along other coastlines, i.e. coastlines with a fine unconsolidated sediment sheet.

Keywords: tidal inlet; bathymetry; seismic VHR; bedrock morphology

1. Introduction

Throughout the world, tidal inlets are of huge environmental and economic importance. They constitute navigation routes to the open ocean, sediment distributors to adjacent shorelines and allow the exchange of nutrients between backbarrier lagoons and the coastal zone. Thus, it is important to understand the evolution of these systems, and be able to predict their behaviour (FitzGerald, 1996). Many tidal inlet studies have been conducted around the world since the beginning of the 20th century, including quantitative

* Corresponding author. Tel.: +33-546-45-72-31; Fax: +33-546-45-82-49.
E-mail addresses: xavier.bertin@univ-lr.fr (X. Bertin), weber@shom.fr (N. Weber), tesson@univ-perp.fr (M. Tesson).

0025-3227/03/$ – see front matter © 2003 Elsevier B.V. All rights reserved.
doi:10.1016/S0025-3227(03)00353-0

approaches by Lecontes (1905) and O'brien (1931). Most of these studies have focused on hydrodynamic processes and meso- to macro-scale evolution (day to year and metre to kilometre; Mehta, 1996), with the result that research topics such as shoreline response to inlet processes, inlet evolution at hyper-scales (1–10 km and year to century scale) or sediment budget questions are poorly understood (Mehta, 1996). Studies of hyper-scale evolution are mostly based on bathymetric data exploitation (FitzGerald, 1984, 1988; Michel, 1997), aerial photographic analysis (FitzGerald, 1982, 1984; Komar, 1996) and, more recently, video monitoring techniques (Balouin, 2001; Morris et al., 2001). These studies rarely allow a detailed tri-dimensional monitoring of bathymetric evolution, but have led to conceptual models that couple tidal channel characteristics with the evolution of adjacent shorelines (FitzGerald, 1984, 1988; Oertel, 1988; Michel and Howa, 1996). In some cases, relations have also been suggested between the location of the tidal channel and the topography of the substratum (Kraft, 1971; Foyle and Oertel, 1992; FitzGerald, 1996; FitzGerald et al., 2002).

This study is focused on Maumusson Inlet, located on the Atlantic coast of France. Understanding the evolution of this tidal inlet is essential because it permits the daily replacement of water of the Marennes–Oléron tidal bay (Fig. 1), the first oyster farming domain in Europe. In addition, adjacent shorelines, that have been experiencing high erosion in the last decades, are also submitted to the high summer flux of tourist population each summer.

It is the purpose of this paper to understand the evolution of this tidal inlet system at hyper-scale. To this effect, an innovative method that combines the exploitation of accurate bathymetric data and very high resolution (VHR) seismic data is proposed. This method has already been used to demonstrate detailed changes of an estuarine sand bank located near the study area (Chaumillon et al., 2002). Firstly, the exploitation

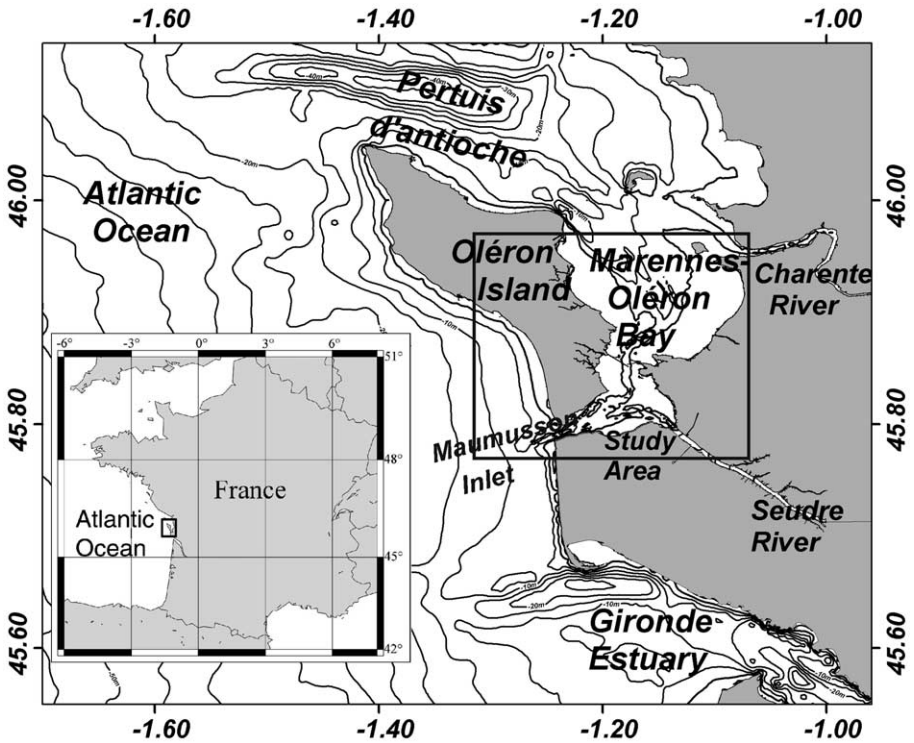

Fig. 1. Simplified bathymethric map and general location of the study area (bathymetric interval is 5 m).

of high quality bathymetric data sets, available since 1824, is used to characterise the hyper-scale morphological evolution of Maumusson Inlet and Marennes–Oléron Bay. The chronology of morphological evolution has enabled us to document strong couplings between the morphological units. Next, VHR seismic investigation has demonstrated relationships between the inlet hyper-scale evolution and the morphology of the Mesozoic substratum. This study offers a conceptual model that includes the inlet, its adjacent shorelines and the tidal bay, and where the bedrock control of the main channel location varies in time. This model could be considered for the development of other inlets emplaced in coastlines characterised by a fine unconsolidated sedimentary sheet.

2. Physical setting

Maumusson Inlet is located in the middle part of the Atlantic coast of France, belonging to a passive continental margin. It separates Oléron Island to the north and Arvert Peninsula to the south. Marennes–Oléron Bay is a 150-km^2 macrotidal bay that is connected to the Atlantic Ocean through Maumusson Inlet to the south and Pertuis d'Antioche to the north (Fig. 1). The intertidal area represents 60% of the bay, mainly consisting of wide mudflats (Gouleau et al., 2000). Two small rivers flow into Marennes–Oléron Bay: the Charente River in the northern part of the bay and the Seudre river in its southern portion. The adjacent shorelines of Maumusson Inlet consist of unconsolidated sediments and are bordered by high aeolian dunes. The Gatseau headland, in the north, corresponds to a 8-km long sandy spit. Three main geomorphologic units can be distinguished in this tidal inlet system, using the terminology introduced by Hayes (1975) (Fig. 2): (1) a well developed ebb delta, confined by the Gatseau sandbank and the Mattes sandbank; (2) a moderately developed flood delta, bordered by the Bry sandbank, the Barat sandbank and the Auger sandbank; and (3) the main tidal channel which corresponds to the so-called 'Pertuis de Maumusson'.

The tide is semi-diurnal ranging from less than 2 m to more than 6 m during spring tides. Associated tidal currents are weak and rotary on the continental shelf (SHOM, 1993), but strong within the inlet (up to 2 m/s; Tesson, 1973), particularly during ebb. The two-connection geometry of Marennes–Oléron Bay with the ocean leads to a strong asymmetry between ebb and flood: the ebb tidal prism is about twice as large as the flood tidal prism (210×10^6 m^3 vs. 120×10^6 m^3, respectively; Tesson, 1973). Freshwater discharge from

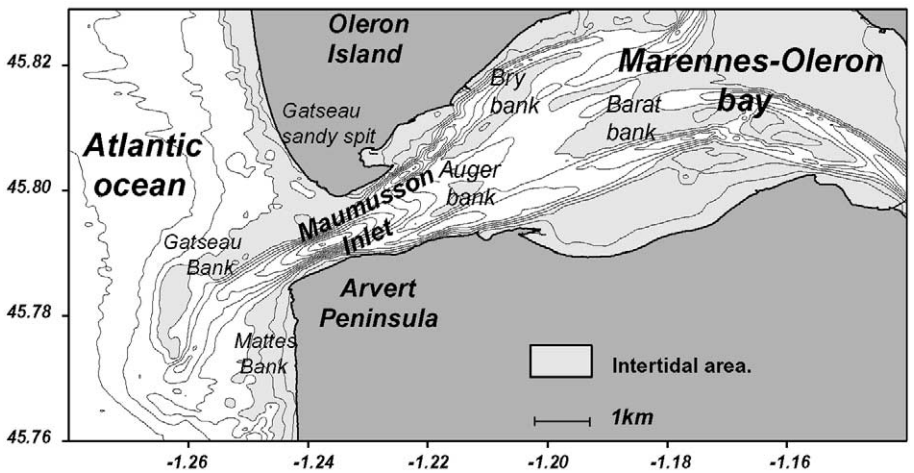

Fig. 2. Detailed bathymetric map of the study area (bathymetric interval is 2 m). Digital elevation model has been made from a 2001 bathymetric survey. The shoreline corresponds to the 1997 shoreline.

rivers is two orders of magnitude less than the tidal prisms: 100 m^3/s for the Charente River and 0.55 m^3/s for the Seudre River (Tesson, 1973).

The yearly average significant wave height is about 1.5 m but wave height can exceed 6 m during storms. The west and northwest directions are predominant, representing more than 56% of the wave climate (LHF, 1994), and inducing a southward net littoral transport. Consequently, the Gatseau sandy spit corresponds to the updrift coast and the Arvert Peninsula to the downdrift coast. Using empirical equations, this net littoral drift has been estimated to be more than 500 000 m^3 (Baxerres, 1978).

According to these hydrodynamic parameters and referring to the terminology of Hayes (1979), Maumusson Inlet is a mixed energy, tide dominant inlet. This tidal dominance is expressed in the large development of the ebb delta, on both sides of the single and deep tidal channel, according to the geomorphic model of Hubbart et al. (1979).

3. Methods and data

3.1. Bathymetric data

Due to the implantation of the national naval dockyard in the Charente River, high quality bathymetric data have been available for the study area since 1824. Bathymetric data from 1824 to 1946 have been extracted from the data base of the Service Hydrographique et Océanographique de la Marine (SHOM) and digitised from the original map using Geographic Information System Arcview. Bathymetric data from 1970 to 2001 have been extracted from the data base of DDE Charente Maritime (Local hydrographic office). All these data have been georeferenced using Arcview software and extensions developed by the SHOM. The local geodesic system New Triangulation of France (NTF) has been chosen with Clarke 1880 as the reference ellipsoid. Two kinds of co-ordinates have then been calculated: geographic co-ordinates for channel and shoreline descriptions and Lambert II for surface and distance calculations. Digital Elevation Models (DEMs) have been developed using Surfer software with a grid spacing of 20 to 200 m, according to the mean initial data sampling. Taking into account corrections and uncertainties, the maximum error margin is 20 m horizontally and 1 m vertically for data taken prior to 1970, and 2 m and 0.1 m, respectively, since 1970. This reliability of measurements was checked through rocky outcrop stability between each survey (Fig. 3).

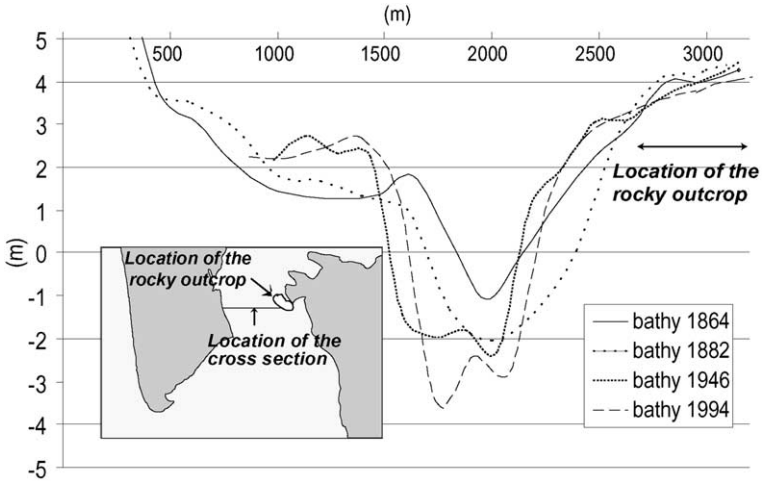

Fig. 3. Superimposition of identical bathymetric profiles recorded at different periods (1864, 1882, 1946 and 1994) on a rocky outcrop we consider to have been stable since 1824. The maximum distance among the four cross sections on the outcrop is less than 0.7 m, which confirms the data accuracy.

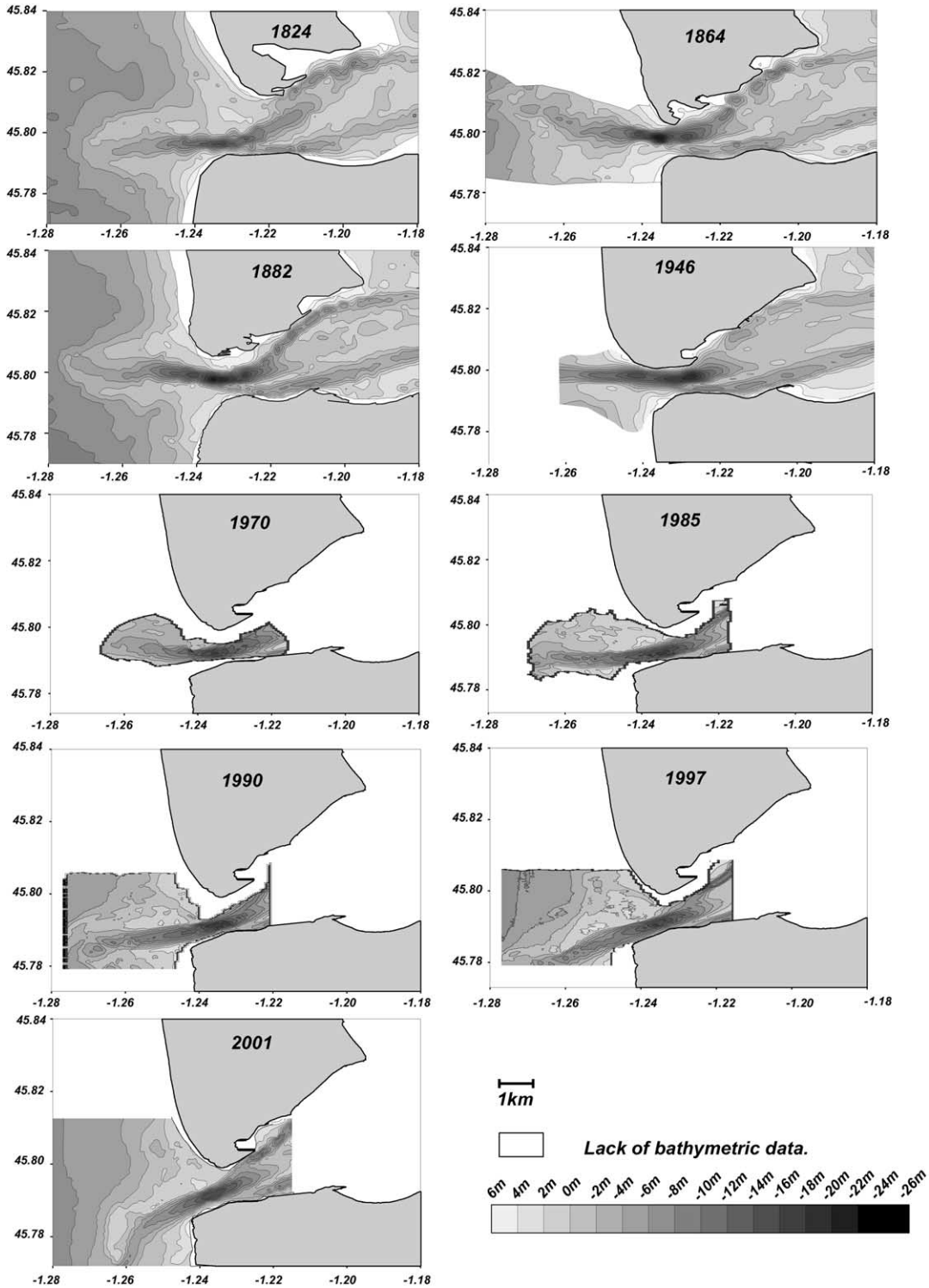

Fig. 4. DEM displaying the evolution of Maumusson Inlet and its adjacent shorelines from 1824 to 2001 (bathymetric interval is 2 m).

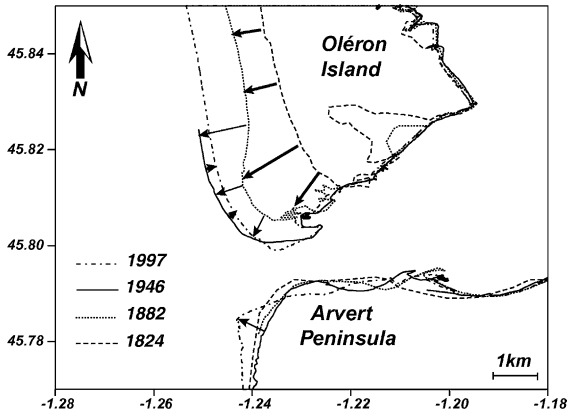

Fig. 5. Evolution of the adjacent shorelines from 1824 to 1946. The 1824, 1882 and 1946 data have been digitised on original maps using the GIS system arcview; the 1997 data arise from aerial photograph analysis.

3.2. Seismic VHR data

Seismic data were collected during the seismic cruise 'Maumusson', conducted in August 2001. Approximately 130 km of profiles covered a high density network (150–1000 m between each profile; see Fig. 8). Two different seismic systems were used: a Sparker source (200–1200 Hz frequency band) associated with a traditional single-channel streamer, and a Boomer source (1–10 kHz frequency band) associated with a line-in-cone receiver (Simpkin and Davis, 1993). These seismic systems provide complementary investigations. Sparker profiling was used for extensive seismic exploration, whereas Boomer profiling was used for restricted and very shallow water targets. The former allows high energy output, penetration into coarse sands and gravels and fast towing speeds while the latter offers high peak frequencies, large bandwidth, high vertical resolution, small offset, fixed geometry and low noise. A differential GPS navigation system with a precision of less than 1 m guaranteed the position accuracy of each seismic trace. Seismic signals were digitised in real time using Delph seismic V.2.01 and processed in three stages: (1) frequency band pass filtering; (2) amplitude correction by applying an automatic gain correction; and (3) stacking of adjacent traces (1–4) depending on lateral facies variations. Seismic profile interpretations were digitised using the Delph system. Time to depth conversion was calculated according to the Maroni (1997) propagation velocity model: 1500 m/s for the water and 1600 m/s for unconsolidated sediments.

4. Results

4.1. Hyper-scale morphological evolution of the inlet and adjacent shorelines

Bathymetric data were used to produce nine DEMs, showing the morphological evolution of the inlet and the adjacent shorelines since 1824 (Fig. 4). The axis of the isobath −10 m was used to describe the channel orientation. Minimum cross-sectional area was calculated using Surfer software (Fig. 5). From 1824, evolution was divided into three major stages (Fig. 4):

(1) From 1824 to 1864 (40 years), the inlet width decreased considerably, from 2 km to less than 1.2 km. The minimum cross-sectional area did not change significantly (around 10 000 m^2; Fig. 6), whereas the channel depth increased from −16 m to −24 m. The channel rotated clockwise from N265° to N275°. During the same period of time, the adjacent shorelines were subjected to major changes (Fig. 7): the updrift coast (Gatseau sandy spit) experienced a progradation of 800 m southwestward (20 m per

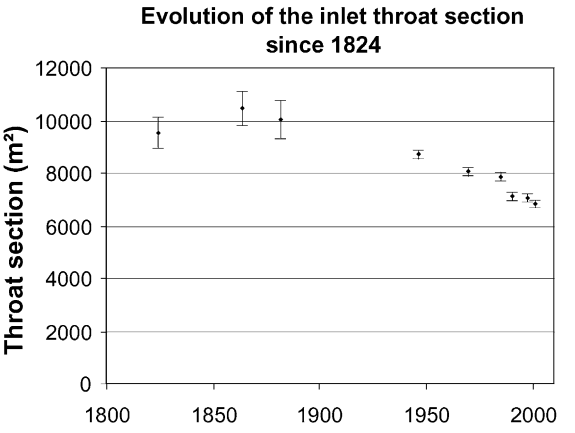

Fig. 6. Evolution of the minimum cross-sectional area since 1824, calculated from DEMs (Fig. 4).

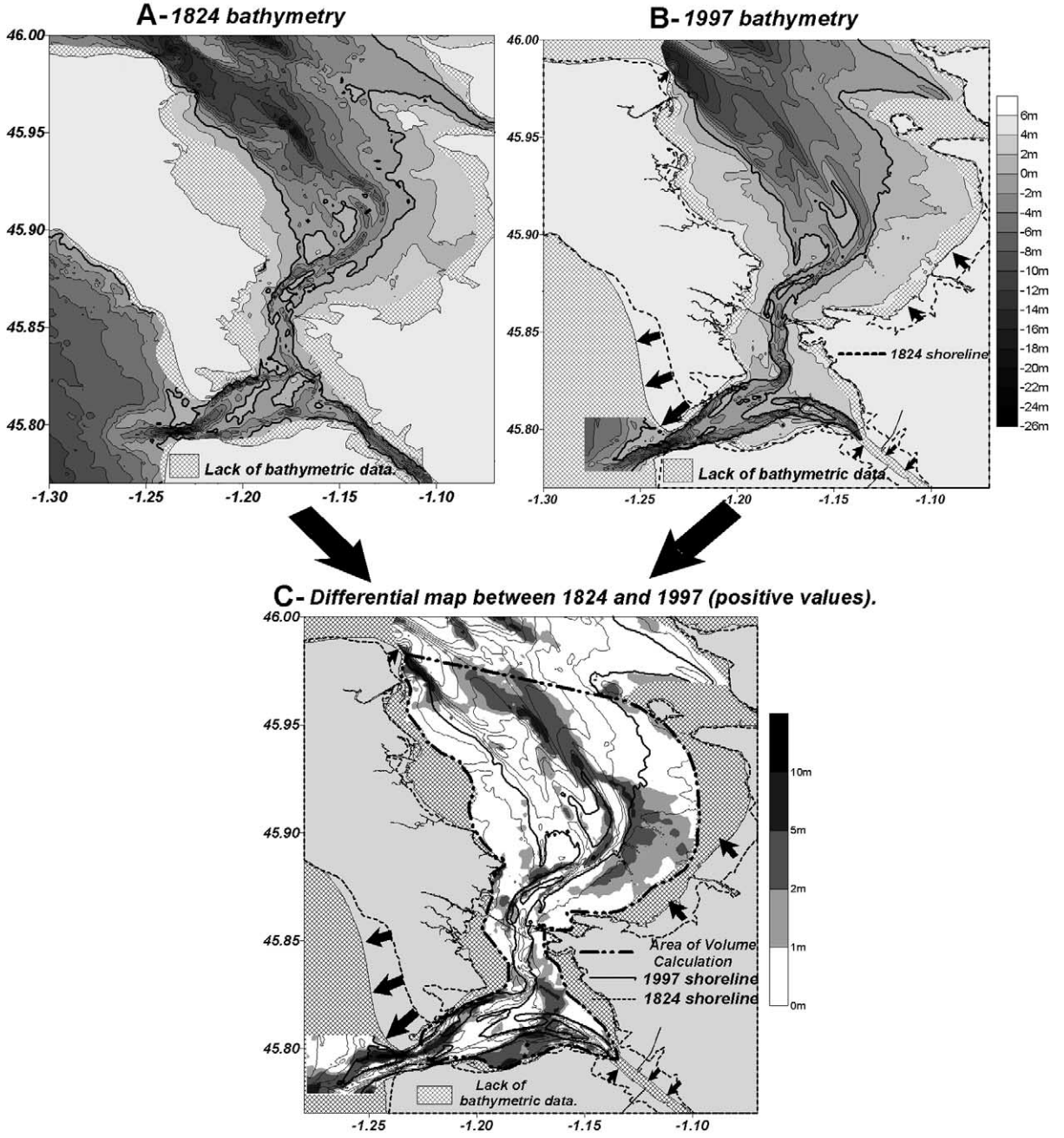

Fig. 7. (A,B) Bathymetric maps in Marennes–Oléron Bay based on digitised charts (1824, SHOM data) and surveys (1995, DDE17 data). The bold line corresponds to the 0-m isobath and the bathymetric interval is 2 m. (C) Bathymetric changes in Marennes–Oléron Bay between 1824 and 1995 evidencing the filling of the bay with sediments. The bathymetric changes are superimposed on the 1995 bathymetry. The boundary of the volume calculation is indicated by the bold dotted line.

year) while the downdrift coast (Arvert Peninsula) shifted 100 m landward.

(2) From 1864 to 1946 (82 years), channel characteristics remained stable: width (1200 m), minimum cross-sectional area around 10 000 m^2, maximum depth around −24 m and orientation N275°. The updrift coast (Gatseau sandy spit) continued to prograde southwestward, but slowed to 6 m/yr (500 m between 1864 to 1946). The drowndrift coast (Arvert Peninsula) remained stable.

(3) From 1946 to 2001 (55 years), the cross-sectional area and maximum depth decreased significantly. The tidal channel shifted southward and its orientation changed from N272° to N232°. The evolutionary tendency reversed in the updrift coast (Gatseau sandy spit), which had experienced erosion since 1960, with an acceleration of erosion rates from 7 m/yr in 1970 to up to 20 m/yr at present. The northern part of the downdrift coast (Arvert Peninsula; Fig. 2) regressed from 400 m southward and progradated 400 m westward.

4.2. Morphological evolution of the tidal bay

To a great extent, Marennes–Oléron Bay experienced accretion between 1824 and 1997 (Fig. 4). Sediment gain occurred in three kinds of areas: (1) close to connections with the ocean (Pertuis d'Antioche to the north and Maumusson Inlet to the south), associated with shoreline progradation; (2) in the eastern and southern parts of the bay where maximum accretion (up to 3 m) occurred in the lower part of intertidal area; and (3) in the wide tidal channel located in the northern part of bay, where sedimentary accretion has locally attained 10 m since 1824.

These two data sets were computed and a volume calculation between 1824 and 1995 DEM (Fig. 3) clearly shows that accretion was dominant in the sediment budget of Marennes–Oléron Bay over the last 171 years: $+106\times10^6 m^3$. We have estimated the corresponding average sedimentation rate to be 0.46 cm/yr. This sedimentation rate estimation is consistent with the results previously obtained from ^{210}Pb measurements on a mudflat located in the eastern part of the bay (Gouleau et al., 2000). This infilling with sediment has led to a decrease in water volume within the tidal bay. We have estimated this decrease in water volume since 1824 to be of the order of 20% for spring tide.

4.3. Inlet internal architecture

Seismic interpretation was based on four criteria following the terminology introduced by Mitchum et al. (1977): (1) identification of key surfaces underlined by reflection terminations: downlap, onlap, toplap, erosion truncation; (2) internal configuration of seismic units; (3) dip and orientation of reflectors; and (4) seismic facies: amplitude, frequency and continuity. Two main seismic units below the seabottom (U0 and U1) were recognised.

4.3.1. Seismic unit Uo

Unit Uo displays strong amplitude, subparallel and low frequency reflectors. The top of this unit exhibits a typically erosional truncation displaying deep (1–25 m) and wide (500–3000 m) incisions. Continuity of these reflectors with coastal rocky outcrops suggests a correspondence with the Mesozoic substratum.

4.3.2. Seismic unit U1

Unit U1 displays two kinds of internal configuration: progradational and subhorizontal reflectors. Progradational seismic packages are identified in three settings: (1) in bedrock incision infills, with apparent southward dipping reflectors (Fig. 8, profiles Maumu01 and Maumu09; Fig. 9 profile Maumu09); (2) in the oceanic part of the inlet, with apparently southward dipping reflectors (Fig. 7, profiles Maumu01, Maumu09 and Maumu10; Fig. 8, profile Maumu9); and (3) in sand banks, topped by the seafloor surface (Fig. 8, profile Maumu12).

4.3.3. Morphology of the Mesozoic substratum

In this preliminary study, the seismic interpretation was focused on the bedrock upper erosional surface morphology. The isobath map for the Mesozoic substratum upper surface has been reconstructed by removal of seismic unit U1 (Fig. 10). This map displays a major incision in the

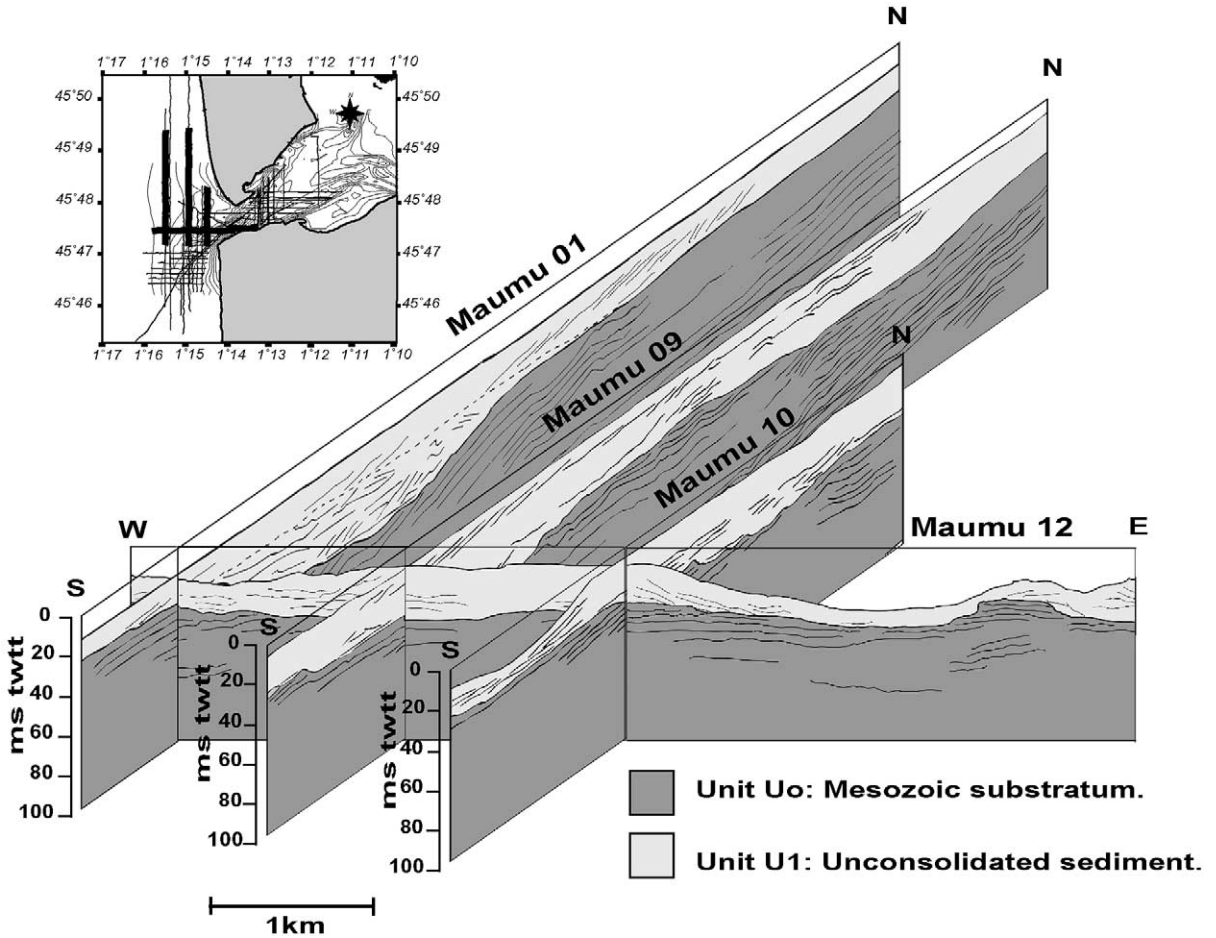

Fig. 8. 3-D diagram built from seismic lines Maumu01, Maumu09, Maumu10 and Maumu12, illustrating the occurrence of a major incision below Maumusson Inlet.

substratum located under the present day inlet, that is elongated toward the sea in a wide and deep trough (1–3 km width and up to 20 m deep relative to the adjacent interfluves). In the shoreward part of the inlet, the incision depth decreased and bifurcated into smaller valleys (300–500 m wide and less than 8 m deep relative to the adjacent interfluves) that were located beneath present day tidal channel.

5. Discussion

Firstly, morphological evolution throughout the last 171 years (1824–2001) suggests strong coupling among the main channel, the bay and adjacent shorelines. Secondly, the morphology of the bedrock substratum together with the chronology of the tidal channel evolution most likely indicate a bedrock control of main inlet channel development. Finally, a conceptual model is proposed, including the main components involved in the development of this inlet system: the main channel, bedrock, bay and adjacent shorelines.

5.1. Coupling between the tidal channel and adjacent shorelines

Morphological changes at Maumusson Inlet display similarity with some of the evolutionary

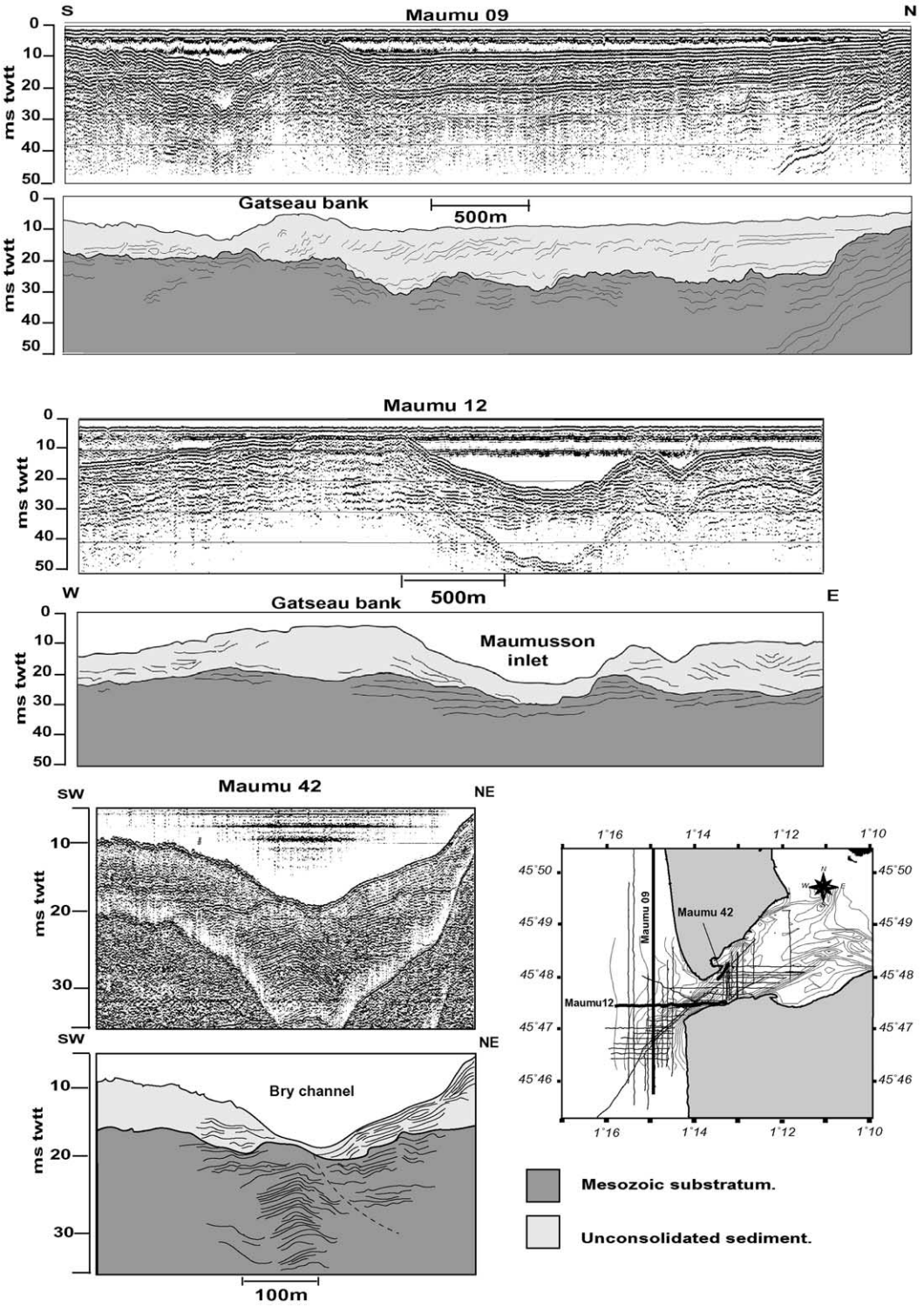
S
Maumu 09
N
ms twtt
0
10
20
30
40
50
Gatseau bank
500m
Maumu 12
W
E
Maumusson
inlet
SW
NE
Maumu 42
Bry channel
100m
1°16
1°14
1°12
1°10
45°50
45°49
45°48
45°47
45°46
Maumu 09
Maumu12
Mesozoic substratum.
Unconsolidated sediment.

features described in previous morphodynamic inlet studies (FitzGerald, 1984; Oertel, 1988; Michel and Howa, 1996). Two main configurations were identified from the DEMs (1964–1946 and 1970–2001).

From 1864 to 1946, the tidal channel characteristics (location, width and minimum cross-sectional area) show little variation and do not evolve significantly. The orientation of the channel (N272–N275°) created a hydraulic obstacle to the southward longshore drift, as described by Todd (1968) in other inlet systems. Deposition of sediment transported by waves may explain the rapid southwestward progradation of the Gatseau sandy spit during this period. The progradation of the shoreline far updrift (8 km for Maumusson Inlet) has been described for similar cases in Florida (Dean and Work, 1993). The protective role of the ebb delta, well developed during this period, may have contributed to the updrift coast construction. Actually, the ebb delta constituted an efficient protection of the coast by causing the waves to break seaward of the inlet, particularly during storm events (FitzGerald, 1996; Mehta, 1996). Evolution of the downdrift coast is less important, nonetheless; we note a moderate northwestward progradation. This could be explained by a local reversal of the longshore drift, due to the southern part of the ebb delta (Fig. 4), causing anticlockwise wave refraction, as suggested by Tesson (1973).

From 1970 to 2001, the tidal channel displays the strongest changes: its maximum depth and minimum cross-sectional area decreased while its axis shifted southward. It can be argued that the new orientation of the channel southwestward provided a less efficient hydraulic obstacle and allowed the bypass of sediments southward. This new configuration, where the sediment is no longer trapped updrift and by-passes downdrift, could explain the beginning of the updrift coast erosion. The increase in updrift coast erosion rate when the channel shifted tends to confirm this hypothesis. On the contrary, this by-pass of sediment downdrift could explain the 400-m westward progradation of the Arvert Peninsula. During the same time, the Mattes sandbank disappeared, and gave way to the new location of the channel. The southward migration of the channel caused the erosion of the northern part of the Arvert Peninsula.

5.2. The causes for the shoaling of the channel

The well known relation that links the minimum cross-sectional area to the tidal prism was first recognised by Lecontes (1905) and refined by O'brien (1931, 1969) and others (Nayac, 1971; Jarrett, 1976; Hume and Herdendorf, 1993; Michel, 1997; Hugues, 2002). This relation is of the form:

$$A = C.\Omega^n \quad (1)$$

where n is a dimensionless value ranging between 0.84 and 1.10 (Jarrett, 1976) and C is a scaling coefficient acquiring the dimensions necessary for dimensional balance in view of the selected exponent (Hugues, 2002).

This relation implies that the inlet throat and the whole inlet channel enlarges or contracts as its tidal prism changes. FitzGerald (1996) has also observed short term variations in throat cross section up to 7% due to predicted changes in the astronomic tidal range. As bathymetric surveys were conducted during spring tides at Maumusson Inlet, the variation in throat cross section evidenced since 1824 (Fig. 6) did not correspond to tidal range changes between each survey. Considering O'Brien's relation (Eq. 1), we rather propose that the decrease in minimum cross-sectional area was related to a long term decrease in tidal prism. Depending on the n exponent value (0.84–1.1), the tidal prism decrease is estimated to be of the order of 30–40% between 1824 and 2001.

As the tidal prism is a function of the tidal range and the morphology of the bay (Stauble,

Fig. 9. Processed seismic profiles Maumu09 and Maumu12 (Sparker profile) and Maumu42 (Boomer profile) and their interpretation. These seismic profiles show the internal architecture of unconsolidated sediment lying on the incised bedrock within the Maumusson Inlet area.

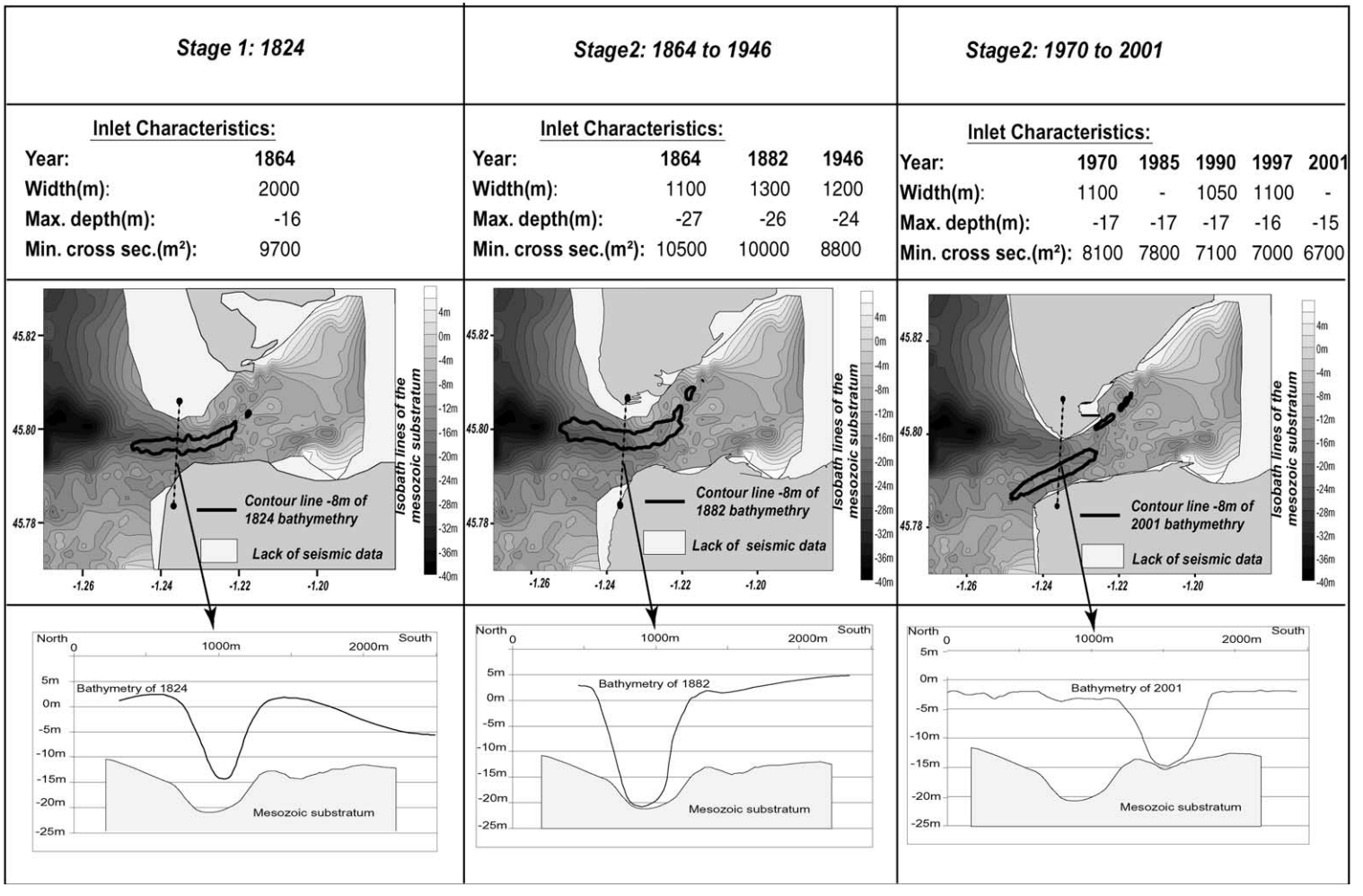

Fig. 10. Superimposition of the main channel (bathymetric line −8 m) at different times on the isobath map of the Mesozoic substratum. The three stages proposed show that the bedrock control varies in time as a function of the channel depth. The isobath map of the Mesozoic substratum corresponds to a DEM obtained from our seismic data.

1993; FitzGerald, 1996), the sediment infilling of Marennes–Oléron Bay (associated with a reduction of its water volume infill of the order of 20%) could directly explain one part of the tidal prism decrease at Maumusson Inlet. But due to its two-connection geometry with the ocean, the relation between water volume infill and tidal prism is non-linear. The strong asymmetry between the ebb and flood tidal prism supports this argument. In addition, it can be postulated that the decrease in water depth, particularly in the northern part of the bay, is responsible for an increase in frictional resistance to tidal wave propagation and a subsequent decrease in tidal flows.

Thus, we infer that the sediment filling in of the bay since 1824 is responsible for a decrease in tidal prism of the order of 30–40%, leading to a decrease in throat section area and a general shoaling of Maumusson Inlet. As a consequence, we postulate the recent shoaling of the inlet could well be irreversible.

5.3. Coupling between the bedrock topography and the location of the channel

The isobath map of the bedrock substratum shows that the inlet was located on a major incision. We believe that this incision corresponds to a segment of a drowned valley. Taking into account its dimensions, it belongs to the large valley class (Ashley and Sheridan, 1994). Its location between the Gironde drowned valley southward (Lericolais et al., 2001) and the Charente drowned valley northward (Weber et al., submitted) suggests that this major incision forms part of the Seudre incised valley (Fig. 1). Combining the bathymetric evolution and our seismic interpretation, we propose three stages of channel evolution.

(1) In 1824, the inlet was wide and moderately deep and the top of the bedrock was under several meters of unconsolidated sediment.

(2) From 1824 to 1946, the strong southward progradation of the Gatseau sandy spit reduced the channel width by half. As the minimum cross-sectional area remained constant during this period, the channel depth increased strongly up to 25 m below sea level, while its orientation rotated from N265° to N275°. At this depth, according to our seismic interpretation, the bottom of the channel became anchored in a previous bedrock incision. We propose that in this configuration, the bedrock topography controlled the new channel orientation (N275°), parallel to the bedrock incision. This bedrock control of the channel orientation and location could explain its remarkable stability against a probably important southward littoral drift, attested to by the fast progradation of the Gatseau sandy spit.

(3) From 1970 to 2001, the decrease in the minimum cross-sectional area was accompanied by a decrease in the maximum channel depth. As a result, the bedrock topography no longer constrained the western part of the channel and allowed it to shift southward, under littoral drift action.

Several studies describe tidal inlets where their development was influenced by antecedent drainage systems and more generally the topography of pre-transgressed landscapes (Kraft, 1971; Sindowsky, 1973; Hume and Herdendorf, 1988; Foyle and Oertel, 1992; Oertel et al., 1992; FitzGerald, 1996, FitzGerald et al., 2002). Thus, Morton and Donaldson (1973) demonstrated that Wachapreague Inlet location (Virginia, USA) coincided with a Pleistocene pre-existing valley and proposed this setting to be responsible for its relative stability. In our study, shallow seismic profiling combined with accurate bathymetric data exploitation brings better insight on relations between inlet development and antecedent drainage systems. In addition, we argue that bedrock control of channel development varies in time as a function of the channel maximum depth.

5.4. Model of the inlet development

The results presented above allow us to propose a two-stage conceptual model for the development of Maumusson Inlet (Fig. 11), explaining relations among the tidal bay, the inlet, the bedrock incision and adjacent shorelines.

During Stage 1 the inlet main channel was deep (>23 m) and anchored in the bedrock incision that imposed its orientation of N275°. Oriented in such a way, the channel created an hydraulic

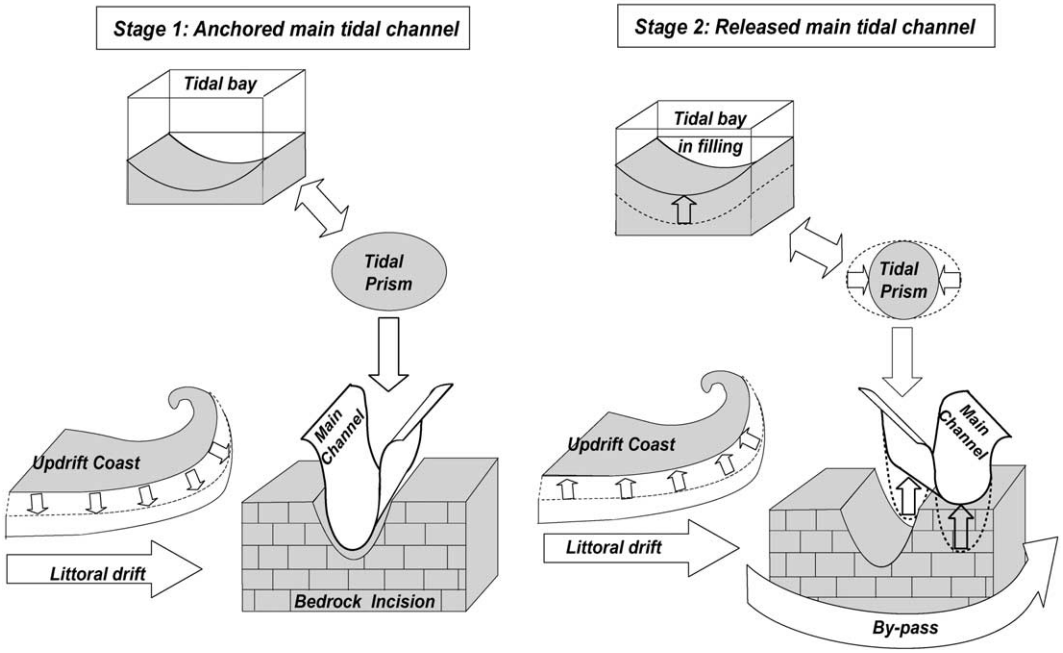

Fig. 11. Two-stages conceptual model, showing relations between the tidal bay, main channel, bedrock and adjacent shorelines.

obstacle interrupting longshore sediment transport and leading to a fast progradation of the updrift coast southwestward.

During Stage 2 the rapid sedimentation in Marennes–Oléron Bay led to a significant decrease in tidal prism, causing the subsequent shoaling of the inlet (maximum depth <16 m). Consequently, the western part of the channel was no longer constrained by the bedrock and shifted southward, allowing sediment to by-pass downdrift while inducing the updrift coast to experience erosion.

Maumusson Inlet is located in a coastal environment where the unconsolidated sediment drape is often reduced due to: (1) large and frequent sea-level oscillations during the last two million years, and (2) moderate crustal motion related to the stable continental margin setting. Such settings are widespread, thus we infer that our model is likely to be applicable to other inlet systems, particularly to those emplaced upon antecedent drainage systems (Kraft, 1971; Sindowsky, 1973; Morton and Donaldson, 1973; Hume and Herdendorf, 1988; Foyle and Oertel, 1992; Oertel et al., 1992; FitzGerald, 1996). This time-varying bedrock control has been demonstrated at Maumusson Inlet because of rapid shoaling of the main channel subsequent to rapid sediment infill in Marennes–Oléron Bay. To a larger extent, we infer that other tidal inlets may have experienced similar stages in their development in the past or could experience them in the future.

6. Conclusions

This work, which combines accurate bathymetric data and VHR seismic profiles, demonstrates the hyper-scale morphologic evolution of a mixed energy inlet system since 1824. It has provided strong evidence of couplings between the main channel, adjacent shorelines and the tidal bay. In addition, shallow seismic investigations have clearly shown that the inlet was located on a major incision of the Mesozoic substratum. Combining this with morphological changes of the inlet, a time-varying bedrock control of main channel development has been unravelled. Finally, a two-stage conceptual model has been proposed, the major points of which are:

(1) The main channel, anchored in a previous bedrock channel, acts as a hydraulic obstacle on littoral drift.

(2) The main channel is not constrained by the bedrock, because it experiences shoaling subsequent to sedimentation in the bay, which then allowed sediment to by-pass downdrift.

This study clearly demonstrates that shallow seismic investigations bring new insight about bedrock control on tidal inlet development.

Acknowledgements

The authors wish to thank DDE 17 (Local hydrographic office) for allowing them to organise the 'Maumussson' seismic cruise. Data treatment was supported by the Service Hydrographique et Oceanographique de la Marine (SHOM). The authors wish to thank sincerely Drs. FitzGerald and Oertel for their very constructive reviews. All their suggestions have improved this paper greatly.

References

Ashley, G.M., Sheridan, R.E., 1994. Depositional model for valley fills on a passive continental margin. In: Dalrymple, R.W., Boyd, R.J., Zaitlin, B.A. (Eds.), Incised Valley Systems: Origin and Sedimentary Sequences. SEPM, Soc. Sediment. Geol., Spec. Publ. 51, pp. 285–301.

Balouin, Y., 2001. Les embouchures mésotidales (tidal inlets) et leur relation avec les littoraux adjacents – exemple de la Barra Nova, sud Portugal. Unpubl. Ph.D. Thesis, Univ. Bordeaux I, 291 pp.

Baxerres, P., 1978. Etude morphologique et sédimentologique de la cote atlantique de la pointe sud d'Oléron a la pointe de la Coubre (France). Unpubl. Ph.D. Thesis, Univ. Bordeaux I, 190 pp.

Chaumillon, E., Gillet, H., Weber, N., Walker, P., Tesson, M., 2002. Evolution temporelle et architecture interne d'un banc sableux estuarien: La Longe de Boyard (littoral Atlantique, France). C.R. Geosci. 334, 119–126.

Dean, R.G., Work, P.A., 1993. Interaction of navigational entrances with adjacent shorelines. J. Coast. Res. 18, 91–110.

FitzGerald, D.M., 1982. Sediment bypassing at mixed energy tidal inlets. Proc. 18th Coastal Engineering Conference, ASCE, Cap Town, pp. 1094–1118.

FitzGerald, D.M., 1984. Interactions between the ebb-tidal delta and landward shoreline: Price Inlet, South Carolina. J. Sediment. Petrol. 48, 227–238.

FitzGerald, D.M., 1988. Shoreline erosional–depositional processes associated with tidal inlets. In: Aubrey, D.G., Weishar, L. (Eds.), Hydrodynamics and Sediment Dynamics of Tidal Inlets. Lecture Notes on Coastal and Estuarine Studies 29, Springer, New York, pp. 186–225.

FitzGerald, D.M., 1996. Geomorphologic variability and morphodynamic and sedimentologic controls on tidal inlets. J. Coast. Res. 23, 47–71.

FitzGerald, D.M., Buynevich, I.V., Davis, R.A., Jr., Fenster, M.S., 2002. New England tidal inlets with special reference to riverine associated inlet systems. Geomorphology 48, 179–208.

Foyle, A.M., Oertel, G.F., 1992. Seismic stratigraphy and coastal drainage patterns in the Quaternary section of the Southern Delmarva Peninsula, Virginia, USA. Sediment. Geol. 80, 261–277.

Gouleau, D., Jouanneau, J.M., Weber, O., Sauriau, P.G., 2000. Short and long-term sedimentation on Montportail–Brouage intertidal mudflat, Marennes–Oléron Bay (France). Cont. Shelf Res. 20, 1513–1530.

Hayes, M.O., 1975. Morphology and sand accumulation in estuaries. In: Cronin, L.E. (Ed.), Estuarine Research, vol. 2. Academic Press, New York, pp. 183–200.

Hayes, M.O., 1979. Barrier island morphology as a function of tidal and wave regime. In: Leatherman, S.P. (Ed.), Barrier Island. Academic Press, New York, pp. 1–28.

Hubbart, D.K., Oertel, G., Nummedal, D., 1979. The role of waves and tidal currents in development of tidal sedimentary structures and sand body geometry: Examples from North Carolina, South Carolina and Georgia. J. Sediment. Petrol. 49, 1073–1092.

Hugues, S.A., 2002. Equilibrium cross-sectional area at tidal inlets. J. Coast. Res. 18, 160–174.

Hume, T.M., Herdendorf, C.E., 1988. A geomorphic classification of estuaries and its application to coastal resources management – a New Zealand example. Ocean Shoreline Management 2, 249–274.

Hume, T.M., Herdendorf, C.E., 1993. Empirical relationships for characterising estuaries. J. Coast. Res. 9, 413–422.

Jarrett, J.T., 1976. Tidal Prism–Inlet Area Relationships. GITI Rep. 3, US Army CERC, Ft. Belvoir, VA, 32 pp.

Komar, P.D., 1996. Tidal inlet processes and morphology related to the transport of sediments. J. Coast. Res. 23, 23–45.

Kraft, J.C., 1971. Sedimentary facies patterns and geologic history of a Holocene marine transgression. Geol. Soc. Am. Bull. 82, 2131–2158.

Lecontes, L.J., 1905. Discussions on 'Notes on the improvement of rivers and harbour outlets in the United States' by Watts, P.A. Trans. Am. Soc. Civ. Eng. 55, 306–308.

Lericolais, G., Berne, S., Fenies, H., 2001. Seaward pinching out and internal stratigraphy of the Gironde incised valley on the shelf (Bay of Biscay). Mar. Geol. 175, 183–197.

LHF, 1994. Estimation des houles résiduelles dans le bassin de Marennes–Oléron. Contrat L.H.F./Ifremer 925526049.

Maroni, C.S., 1997. Détermination automatique de la stratigraphie des fonds marins à l'aide d'un sondeur de sédiments. Unpubl. Ph.D. Thesis, UBO University, 262 pp.

Mehta, A.J., 1996. A perspective on process related research needs for sandy inlets. J. Coast. Res. 23, 3–21.

Michel, D., Howa, H.L., 1996. Morphodynamic behaviour of a tidal inlet system in a mixed energy environment. Phys. Chem. Earth 22, 339–343.

Michel, D., 1997. Evolution morphodynamique d'un littoral sableux situé à l'aval d'une embouchure lagunaire. Unpubl. Ph.D. Thesis, Univ. Bordeaux I, 161 pp.

Mitchum, R.M., Vail, P.R., Sangree, J.B., 1977. Stratigraphic interpretation of seismic reflection patterns in depositional sequences. In: Payton, C.E. (Ed.), Application to Hydrocarbon Exploration. Am. Assoc. Pet. Geol. Bull., Tusla, pp. 117–133.

Morris, B.D., Davidson, M.A., Huntley, D.A., 2001. Measurement of the response of a coastal inlet using video monitoring techniques. Mar. Geol. 175, 251–272.

Morton, R.A., Donaldson, A.C., 1973. Sediment distribution and evolution of tidal deltas along a tide dominated shoreline, Wachapreague, Virginia. Sediment. Geol. 10, 285–299.

Nayac, I.V., 1971. Tidal Prism Area Relationship in a Model Inlet. Technical report HEL 24–1, Hydraulic Engineering Laboratory, University of California, Berkeley, CA.

O'brien, M.P., 1931. Estuary tidal prism related to entrance area. Civil Eng. 1, 738–739.

O'brien, M.P., 1969. Equilibrium flow areas of inlets on sandy coasts. Waterways and Harbors Div. Proc. of 13th Coast. Eng. Conf., pp. 761–780.

Oertel, G.F., 1988. Processes of sediment exchange between tidal inlets and barrier islands. In: Aubrey, D.G., Weishar, L. (Eds.), Hydrodynamics and Sediment Dynamics of Tidal Inlets. Springer, New York, pp. 186–225.

Oertel, G.F., Kraft, J.C., Kearney, M.S., Woo, H.J., 1992. A rational theory for barrier-lagoon development. In: Quaternary Coasts of the United States Marine and Lacustrine Systems. SEPM Spec. Publ. 48, 77–87.

Service Hydrographique et Océanographique de la Marine (SHOM), 1993. Courants de marée de la cote ouest de france. Imprimerie de l'EPSHOM, Brest, 42 pp.

Simpkin, P.G., Davis, A., 1993. For Seismic profiling in very shallow water, a novel receiver. Sea Technol. 34, 21–28.

Sindowsky, K., 1973. Das ostfriesische Kustengebiet. Sammlung geologischer Fuührer 57, 103 pp.

Stauble, D.K., 1993. An overview of southeast Florida inlet morphodynamics. J. Coast. Res. 18, 1–27.

Tesson, M., 1973. Aspects dynamiques de la sédimentation dans la baie de Marenne Oléron (Charente-Maritime). Unpubl. Ph.D. Thesis, Univ. Bordeaux I, 128 pp.

Todd, T.W., 1968. Dynamic diversion – influence of longshore current–tidal flow interaction on chenier and barrier island plains. J. Sediment. Petrol. 38, 734–746.

Weber, N., Chaumillon, E., Tesson, M., Garland, T., in prep. Morphology and internal organication of the outer segment of a mixed tide and wave dominated incised valley revealed by pseudo 3D seismic profiling: The paleo-Charente River.